The Effect of Loads in Molecular Communications

Cameron McBride*, *Student Member, IEEE,* Rushina Shah*, *Student Member, IEEE,*
and Domitilla Del Vecchio, *Senior Member, IEEE*

(Invited Paper)

***Abstract*—The ability of cells to sense and respond to their environment is encoded in biomolecular reaction networks, wherein information travels through processes such as production, modification, and removal of biomolecules. Recent advances in biotechnology have made it possible to re-engineer these physical processes to the point where synthetic biomolecular circuits can be inserted into cells to program cell behavior for useful functionalities. These circuits are often designed in a bottom-up fashion with smaller components connected to form complex systems. In a bottom-up approach to design, it is highly desirable that circuit components behave modularly, that is, that the input-output behavior of a module characterized in isolation, remains unchanged when the context changes. Unfortunately, due to the physical processes by which information is communicated from one biomolecular circuit module to the other, lack of modularity is often a problem. In fact, the input-output behavior of a module depends on both direct connectivity to other modules, due to loading effects, and indirect connectivity arising from loads applied to shared cellular resources. In this review, we summarize published work illustrating how the means of molecular communication lead to these problems. Specifically, we review the concept of retroactivity, which has been proposed to capture loading problems within a "signals and systems" framework, allowing for engineering solutions that restore modularity.**

***Index Terms*—modularity, communication, synthetic biology, biomolecular systems**

I. Introduction

LIVING cells possess the ability to sense, process, react to information from their environment, and to communicate with other cells [1–4]. Specifically, cells sense environmental stimuli such as temperature, pressure, or nutrients by means of signal transduction cascades, wherein proteins become covalently modified in response to signals and, once they are modified, they can act on gene expression by enhancing or inhibiting the production of other proteins [5]. The process of gene expression regulation can create highly sophisticated circuitry important for decision making [6–8] and enables the cell to "compute" and respond to environmental stimuli. In turn, the molecular processes constituting signal transduction and gene expression regulation can be utilized to engineer and design synthetic biological circuits, which may be inserted into cells to 'program' cellular behavior [9]. Examples of early synthetic genetic circuits constructed include the toggle switch [10], which is a system capable of storing two memory states to enable binary decisions, and the repressilator, which is an oscillator that can be used as a clock [11]. The field of synthetic biology has flourished since these early circuits continuing to the present. Today, cells may be engineered for specialized tasks with far-reaching applications in fields such as medicine [12, 13], the environment [14], or energy [15, 16]. For a recent review on synthetic biology, the reader is referred to [17].

The design of synthetic biological circuits largely relies on a bottom-up approach, which starts from building simple functional modules that are then assembled together to build larger, more complex systems [18]. Thus modularity, which is the property where the input-output behavior of a system does not depend on surrounding systems, is highly desirable. Modularity allows different modules to be designed and characterized in "isolation" first, and then combined to form larger systems that are capable of performing various complex tasks. While several functional modules have been successfully created [10, 11, 19, 20], the ability to combine these modules to design complex circuits has been hampered by their lack of modularity. There are many reasons why modularity fails [21], and analyzing and overcoming several of these factors requires a system-level understanding of how signals are processed and communicated through biomolecular reactions.

In this work, we focus on this system-level understanding and delve into a well studied cause of lack of modularity in biomolecular networks: the effect of loads. In biomolecular networks, modules are connected to each other via biochemical reactions, that is, molecular species in an upstream module (the module that sends information) react with species in a downstream module (the module that receives information). These reactions result in an added reaction flux to the dynamics of the upstream module which were not present in the absence of the downstream module. Thus, the behavior of the upstream module changes in the presence of a downstream module. As a consequence, the signal being communicated from a sender (upstream module) to a receiver (downstream module) is changed by the presence of the receiver module. This loading effect has been formally analyzed through the concept of retroactivity–the signal that travels from a downstream module to an upstream module–capturing the change in dynamics of the upstream module upon connection to the downstream module [22]. In this paper, we review how loads on an upstream module arise due to direct connectivity to a downstream module with a focus on experimentally tested work by delving into the molecular mechanisms that allow modules to communicate [22–25]. We will then review both the direct effects of such loads on an upstream module and the indirect connectivity that arises among multiple downstream modules when these share a common upstream module. The latter phenomenon is especially relevant in synthetic genetic circuits

C. McBride, and R. Shah, and D. Del Vecchio are with the Mechanical Engineering Department, Massachusetts Institute of Technology, Cambridge, MA, 02139 USA, email: cmcbride@mit.edu, rushina@mit.edu, ddv@mit.edu.
* Co-first author.

This work was supported by the National Science Foundation Expeditions Award No. 1521925.

because all circuit modules share one common upstream module–the module that produces the resources required for gene expression, chiefly RNAP and ribosomes [5, 26, 27].

Similar lack of modularity has been encountered in engineering fields, most notably in electrical engineering. In fact, impedance problems, where the output voltage of an upstream circuit changes upon connection to a downstream circuit, are at the core of electrical circuit design [28]. The study of these problems led to foundational results, such as Norton's and Thévenin's theorems, which allow designers to compose systems by taking impedance effects into account [28]. The design of negative feedback electrical circuitry led to the ability to insulate an upstream circuit module from a downstream one and enabled large-scale integrated circuits with the advent of the op-amp [28]. This review describes how similar problems arise when communication between two modules occurs through molecular reactions. It further details engineering solutions that have been implemented so far, mostly relying on the design of biomolecular feedback systems, in order to recover modularity [22, 29–33].

This paper is organized as follows. Section II provides an introduction to the physics of the core components of synthetic biological circuits. Section III describes retroactivity and its consequences, and Section IV describe its effects in a resource sharing context. Section V describes the efforts to characterize retroactivity, and Section VI illustrates the concept of feedback design and demonstrates practical applications to restore modularity in synthetic biology. We conclude with Section VII.

II. The Physics of Biomolecular Circuits

In the design of biomolecular circuits, core cellular processes are utilized and composed together within a network [17, 18]. Nodes of this network are defined as the dynamical processes taking one or more proteins as input and giving a protein as output. These processes include protein production through transcription and translation, their regulation by other proteins, and protein covalent modification, wherein the activity of a protein is modified through various means such as phosphorylation (Fig. 1) [5, 34]. The connection of nodes through output-to-input assignments creates a biomolecular circuit. Example circuits include oscillators [11], toggle switches [10, 19] and logic gates [20]. These circuits can then be connected to create more sophisticated systems capable of sensing, e.g. cancer identification [35] or biohazard detection [14]; actuation, e.g. periodic drug release [12] or cancer immunotherapy [13]; or biofuel production [15, 16], among others. Additionally, synthetic biomolecular circuits may be used to enable molecular communication systems whereby signals may be passed between distinct cells using engineered sender and receiver circuits [36–41]. In this section, we introduce the main biological processes used to create biomolecular circuits [5, 34].

A. Background on Biological Processes

In a cell, proteins are important signal-carrying molecules. Therefore the dynamics of protein production are an important driver of the dynamics of biomolecular networks. The process of protein production is a two step process. First, an mRNA molecule is created from DNA by the process of transcription (TX). Next, a protein is produced using this mRNA by the process of translation (TL). Key cellular resources involved in these processes are RNA polymerases (RNAP), which bind to the DNA and initiates transcription, and ribosomes, which bind to the mRNA and perform translation. These steps make up the TX/TL process, whose output is the protein produced (Fig. 1a). Other proteins may act as an input to the TX/TL process by binding to DNA, resulting in a change in the rate of transcription. If the input increases the rate of transcription, the input is called an activator; while if an input decreases the rate of transcription, it is called a repressor. Once proteins are formed, they may also undergo post-translational covalent modifications (for example in the presence or absence of signals from the environment). One important example of such a modification is phosphorylation, where a phosphate group is attached to the substrate protein. This process is catalyzed by an enzymatic protein called the kinase. The phosphorylated protein is then typically dephosphorylated (removal of the phosphate group), by means of an enzymatic protein called the phosphatase. These processes form the phosphorylation-dephosphorylation cycle, a common example of a signaling cycle (Fig. 1c).

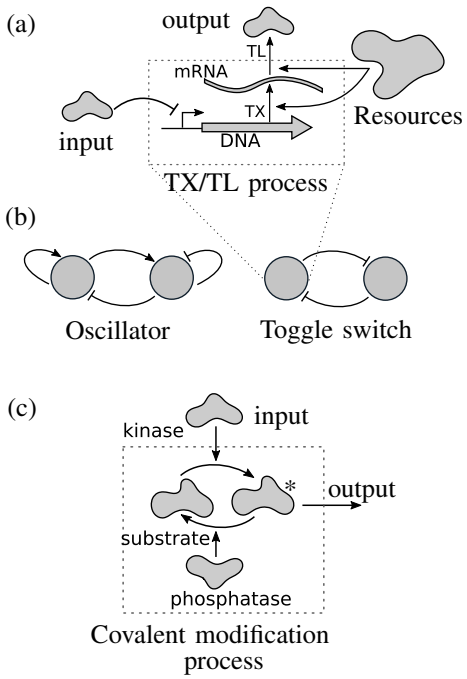

Fig. 1. Diagram of core processes in a biomolecular network. (a) The TX/TL process takes a protein input, which binds to the DNA. This DNA then produces a protein using cellular resources. (b) TX/TL processes can be connected whereby the output of one process activates (→) or represses (⊣) the transcription rate (TX) of another process. Multiple TX/TL processes may be connected to form circuits such as an oscillator [11] or the toggle switch [10]. (c) The covalent modification process takes a protein (kinase) as input, which acts to catalytically modify the substrate protein. The modified protein is also de-modified enzymatically by the phosphatase, forming the covalent modification cycle process. The output of this process may, for example, be the modified protein.

B. Mathematical Modeling of Biomolecular Processes

The TX/TL and phosphorylation-dephosphorylation processes may be modeled through biomolecular reactions between proteins and DNA. Assuming that molecular counts are sufficiently high and the system is well-mixed so that number of molecules can be quantified through molecular concentration, ordinary differential equation (ODE) models may be used to describe biomolecular processes based on reaction-rate equations, which are derived from first principles using the law of mass action [5]. In general, we represent the concentration of a molecule z as z. Consider a process with input protein(s) u and output protein y. This process can be described by the set of ODEs

$$\dot{\mathbf{x}} = f(\mathbf{x}, u) \tag{1a}$$

$$y = g(\mathbf{x}), \tag{1b}$$

where $\mathbf{x}$, is a vector of concentrations of internal states to the process, u is the concentration of the input to the process, f gives the process dynamics derived from the reaction-rate equations, y is the concentration of the output of the process, and g is the output function. Often, model reduction may be used to reduce the dimensionality of the process dynamics to one state and then the process dynamics may be written as a single ODE.

In the case of TX/TL processes, the process dynamics may be reduced to the dynamics of the output protein given as

$$\dot{y} = H(u) - \gamma y, \tag{2}$$

where u is the input to the process, $H(u)$ is the rate of production of the protein y, and γ is the decay rate of protein y. For a single input process, the rate of protein production is modeled using Hill functions [42] of the form

$$H(u) = \frac{\alpha + \beta u^n}{1 + u^n}, \tag{3}$$

for activation, and of the form

$$H(u) = \frac{\beta}{1 + u^n}, \tag{4}$$

for repression. Here, α represents the basal production rate of the protein, β represents the maximum rate of production, and n represents the cooperativity of the input protein u. These functions may be naturally extended to capture multiple input systems where the additional inputs appear in both the numerator and denominator if the input is an activator and only appear in the denominator if the input is a repressor. More details regarding the modeling of TX/TL process and covalent modification process are given in Appendices A and C, and in [5].

As previously mentioned, in a biomolecular network, a node is defined as a dynamical process, such as TX/TL or phosphorylation-dephosphorylation, that takes one or more proteins as inputs and gives one protein as an output. For example, the input to a TX/TL process may be proteins that activate or repress the transcription rate of the node (Fig. 1a). Each node is labeled with its output protein. These nodes can interact with each other, where the output of one node is the input to another node, forming the edges of the network. For example, when an upstream TX/TL node with output protein y is connected to a downstream TX/TL node, the protein y reversibly binds with the DNA of the downstream node [43]. Once bound, the protein-DNA complex either enhances the production of the downstream node's protein (in the case of activation, resulting in the rate of production of the downstream protein being given by (3)), or weakens it (in the case of repression, resulting in rate of production of the downstream protein being given by (4)).

The graph of a genetic circuit (e.g. in Fig. 1b) can be drawn as follows. Given two proteins y_i and y_j, if y_i is the input for y_j and y_i activates the TX of y_j, then a positive edge is drawn from the node representing y_i to y_j with "$\rightarrow$". If the interaction is repression, then a negative edge is drawn from y_i to y_j, represented by "$\dashv$". For example, the oscillator network in Fig. 1b is a network with two nodes: the first node activates itself and the second node, while the second node represses itself and the first node. The graph of a genetic circuit is a convenient way to represent the topology of the circuit. This graph can help give insight into the possible behaviors of the circuit, such as the possibility for multiple equilibria, although the exact behavior of the system is dependent on both the parameters and the network topology [5, 44].

The input to a phosphorylation-dephosphorylation process is usually the kinase that enzymatically catalyzes the phosphorylation reaction (Fig. 1c). When an upstream node with output protein y is connected to a downstream phosphorylation cycle node, protein y reversibly binds to a protein belonging to the downstream node to, for example, enzymatically phosphorylate it. In this way, dynamical processes make up the nodes of a biomolecular network, and reversible binding reactions between molecules of the two nodes make up the edges.

In the remainder of this paper, we define a module as any collection of one or more nodes of a biomolecular system, for example the oscillator and toggle switch in Fig. 1b. Modules are connected to form larger circuits through output-to-input connections, where the output of nodes in the upstream module (sender) is taken as an input by nodes in the downstream module (receiver).

III. Biological Loading and the Concept of Retroactivity

This section describes the problem of loading in biomolecular circuits and the concept of retroactivity to capture loads within a formal systems and signals framework. Specifically, we illustrate how communication of information from an upstream module to a downstream module always implies a change in the signal being transmitted [23, 45]. We start by demonstrating this problem through a brief example. The activator-repressor clock of [46] is a genetic oscillator built of two nodes: an activator node with protein A and a repressor node with protein R. Protein A activates itself and R, and protein R represses A, as shown in Fig. 2a. An ODE model of this system can be derived using the modeling tools shown in Appendix A, which give that the rate of production of A is $H_A(A,R) = \frac{\alpha_1 + \beta_1 A^{n_1}}{1 + A^{n_1} + R^{n_2}}$ and the rate of production of R is $H_R(A,R) = \frac{\alpha_2 + \beta_2 A^{n_1}}{1 + A^{n_1}}$ [47, 48]. For certain parameters,

this clock shows oscillations. However, when the activator is taken as an input to a downstream TX/TL process (Fig. 2b), the oscillations of the clock are quenched (Fig. 2c), and the module fails to communicate the oscillating signal to the downstream node [48–50]. This failure of the upstream module is due to the load that the downstream node applies to the clock, as we demonstrate next by detailing how this molecular communication occurs.

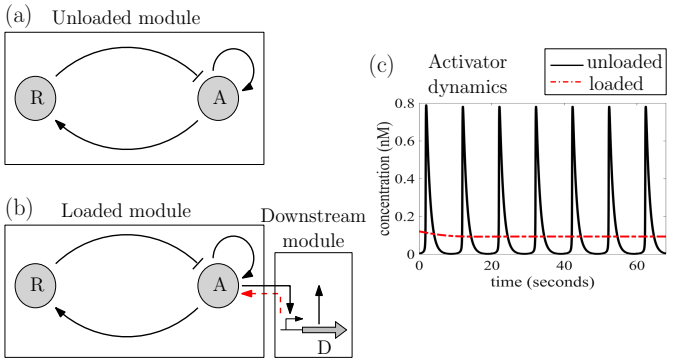

Fig. 2. Effect of direct retroactivity on the activator-repressor clock. (a) The clock in isolation (unloaded module). (b) The clock once its output is used as an input to a downstream module (loaded module) to either activate or repress the TX of a protein. (c) The loaded module fails to oscillate. Details regarding the equations and parameters used in the simulations are given in Appendix A.

Consider a simple genetic circuit, consisting of an upstream TX/TL process with output protein y. The rate of production of y is denoted by $\alpha(t)$ and can, in general, represent any regulatory function such as H_A of node A of the clock (Fig. 2a), and y may be, for example, protein A of the clock. The protein y decays with rate γ, and thus the ODE governing the concentration y of y is

$$\dot{y} = \alpha(t) - \gamma y. \tag{5}$$

This upstream module (sender) is then connected to a downstream TX/TL node (receiver) by protein y reversibly binding to the DNA sites D of the downstream system, as described in Section II. The reactions for this reversible binding are given by

$$\mathrm{y} + \mathrm{D} \underset{k_{\text{off}}}{\overset{k_{\text{on}}}{\rightleftharpoons}} \mathrm{C}, \tag{6}$$

where k_{on} and k_{off} are the binding and unbinding rate constants, respectively, and C is the protein-DNA complex. This additional binding-unbinding reaction results in an additional reaction flux on y, which changes the dynamics of y. The ODE model governing the dynamics of the connected system is

$$\begin{aligned} \dot{y} &= \alpha(t) - \gamma y \underbrace{\boxed{-k_{\text{on}} y D + k_{\text{off}} C,}}_{s} \\ \dot{C} &= k_{\text{on}} y D - k_{\text{off}} C, \end{aligned} \tag{7}$$

where the total concentration of DNA sites $D_T = D + C$ is conserved. The additional reaction flux s is named retroactivity [22, 51], effectively representing a signal that enters the upstream system dynamics (the sender) once this system is connected with a downstream module (the receiver, with DNA D).

The above mechanism of reversible binding for communication between modules provides a physical explanation for why the oscillations in the clock shown in Fig. 2a may be affected when the clock is connected to a downstream module. While in the isolated case, the dynamics of A are only determined by the regulatory interactions between A and R, once the clock is connected to the downstream module (Fig. 2b), these dynamics are influenced by the fact that A must also bind to sites in the downstream module and is therefore available to the regulatory interactions constituting the upstream module.

Reversible binding reactions are typically orders of magnitude faster than protein dynamics ($k_{\text{off}} \gg \gamma$) and, therefore, timescale separation has been utilized to reduce (7) to a simpler form that allows qualitative conclusions about the effects of retroactivity s on the transmitted signal y. Specifically, (7) may be written in standard singular perturbation form [52], with slow variable $z = y + C$, and fast variable C and small parameter $\varepsilon = \gamma/k_{\text{off}}$. Then, the dynamics of the slow variable are $\dot{z} = \alpha(t) - \gamma y$ and the dynamics of the fast variable are $\varepsilon \dot{C} = \gamma y K_D (D_T - C) - \gamma C$, where $K_D = \frac{k_{\text{off}}}{k_{\text{on}}}$ is the dissociation constant. By letting $\varepsilon \to 0$, we have that $C = \frac{D_T y}{y + K_D}$. Then, $\dot{z} = \dot{y} + \dot{C} = \left(1 + \frac{\partial C}{\partial y}\right) \dot{y} = \alpha(t) - \gamma y$. Then, solving for $\dot{y}$, the reduced dynamics of y become

$$\dot{y} = \frac{1}{1 + \boxed{R(y)}} (\alpha(t) - \gamma y), \tag{8}$$

where $R(y) = \frac{\partial C}{\partial y} = \frac{D_T / K_D}{(y/K_D + 1)^2}$ is a measure of the retroactivity applied by the downstream module to the upstream module. Since $R(y) > 0$, (8) implies that retroactivity slows down the dynamics of the output y. That is, signal transmission is slowed down by the presence of the downstream receiver module. This explains why the load to the activator of the clock in Fig. 2 quenches the oscillations. The activator-repressor clock oscillations rely on having a strong activator and a weak repressor [48–50]. The retroactivity that the downstream node applies to the activator slows down its dynamics, making the effective activation weaker, thus quenching the oscillations of the clock.

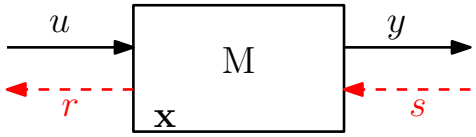

Fig. 3. A module M with input u, output y, and state variable $\mathbf{x}$. The red dashed arrows denote the retroactivity signals arising from interconnection to upstream and downstream modules, respectively. Signal s is named retroactivity to the output and captures the added reaction fluxes that enter the dynamics of M once it is connected to its downstream systems. Signal r is called the retroactivity to the input and captures the "load" that module M is exerting on the upstream system that gives the input u.

Fig. 3 shows a system concept with retroactivity that was proposed in [22] to more rigorously capture the problem of loads and to make this problem amenable of theoretical solutions (Section VI). The retroactivity signal that affects the output of the module M due to its interconnection with

downstream modules is called retroactivity to the output, denoted by s. Due to the retroactivity to the output s, any time module M (sender) is connected to its intended downstream systems (receivers), the information communicated to these systems through y is changed since s affects the dynamics (and therefore the output y) of M. Similarly, the retroactivity signal that module M transmits to upstream modules from which it receives an input u is called retroactivity to the input, denoted by r. Due to retroactivity to the input r, module M changes the information it receives from its upstream system (sender).

The effect of retroactivity was experimentally demonstrated in synthetic genetic circuits in [23] by a theoretical study combined with *in vivo* experiments. Here, retroactivity s resulted in a sign sensitive delay in the output y of the upstream system. Additional combined theoretical and *in vitro* experimental studies demonstrated that similar effects of retroactivity are also seen in signaling systems [24]. Retroactivity was also shown to affect the steady state and input-output response curves $y(u)$ of signaling circuits [25, 53, 54] and gene regulatory networks [55–58].

A plethora of computational studies have investigated the effects of retroactivity on different circuit topologies [59–62]. Fig. 4 shows some example topologies discussed here. For instance, when an upstream module (sender) has multiple downstream modules (receivers), a perturbation in any one of these receivers is transmitted to the rest of the receivers via the retroactivity to the output (Fig. 4a). This has been shown for signaling cycles where downstream cycles that share an upstream kinase (input) behave such that when one cycle is perturbed, the signal is transmitted to the other cycle via retroactivity to the common upstream system [59]. Conversely, multiple upstream sender modules that transmit information to a common receiver module can also become coupled due to the effect of retroactivity [60] (Fig. 4b). Thus, information can be transmitted between modules that were not orignally intended to communicate. Furthermore, information transmission becomes naturally bi-directional since upstream-to-downstream signal propagation can occur only if there is a backward flow of information through the retroactivity signals. This receiver-to-sender backward information flow has been demonstrated, in particular, in signaling cascades [61–63].

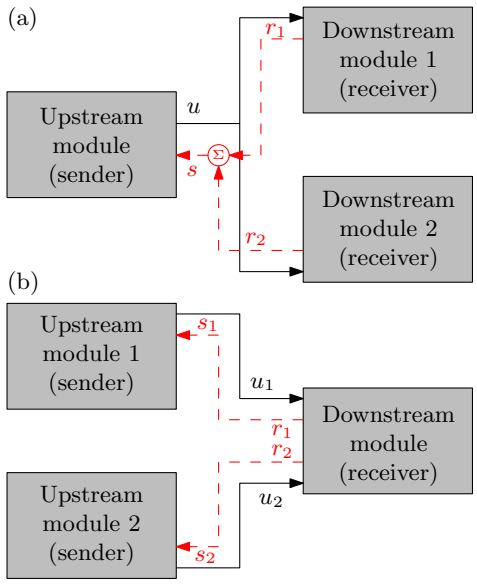

Fig. 4. Effect of retroactivity on example sender/receiver arrangements. (a) When an upstream sender module has multiple downstream receiver modules, a perturbation in one of the receiver modules can be transmitted to the other receiver modules due to retroactivity r_1 and r_2 (dashed red signal). (b) When a downstream receiver module takes inputs from two upstream sender modules, information transmitted by one of the upstream sender modules is "sensed" by the other upstream sender module due to retroactivity to the output s_1 and s_2 transmitted by the common downstream receiver module (dashed red signal).

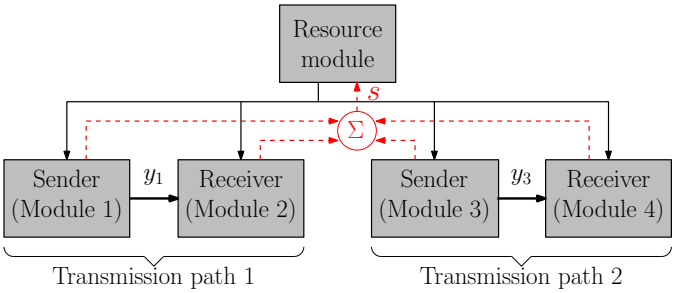

Fig. 5. Downstream modules change the dynamics of the upstream module by retroactivity. Here s denotes the retroactivity to the output of a given module. When an upstream module, such as a pool of common resources, drives multiple downstream modules, the downstream modules act in series, such that the retroactivity to the output of the upstream module is the (scaled) sum of the retroactivity to the input of each of the downstream modules.

IV. Consequences of Retroactivity in Systems with Resource Sharing

All TX/TL processes (Section II), which involve the expression of a protein from a DNA template, require cellular enzymes for the TX and TL processes to occur. These enzymes, chiefly RNAP for TX and ribosomes for TL [5], are shared among all TX/TL processes. Therefore, we can view all genetic modules as having a common upstream system: the cellular process producing the resources required for gene expression. This common upstream "sender" module is subject to retroactivity by its downstream modules according to the arrangement of Fig. 4a. This implies that the communication of information that occurs along seemingly uncoupled transmission paths will, in fact, become coupled (Fig. 5).

A. Effect of Retroactivity on Networks

We consider the situation shown in Fig. 5, where the "upstream" module (resource module) is a system that produces the pool of cellular resources required for gene expression such as RNAP or ribosomes. The retroactivity signal from any downstream module to the resource module affects all other modules since all modules receive an input from the resource module. These retroactivity effects may affect the properties of a communication network in undesirable ways. We demonstrate this concept by capturing the dynamics of the resource module using the system in Fig. 5 as an example. We assume for simplicity that there is one key resource required for gene expression, which has been shown to be a valid assumption in *E. coli* [27]. Let D_i represent the DNA of the

ith node, R represent the resource, C_i the complex formed by DNA and resource, and y_i the protein produced by the ith module. Then, the reactions describing the system may be written as

$$\mathrm{D}_i + \mathrm{R} \underset{d_i}{\overset{a_i}{\rightleftharpoons}} \mathrm{C}_i \xrightarrow{k_i} \mathrm{D}_i + \mathrm{R} + \mathrm{y}_i$$
$$\mathrm{R} \underset{\alpha}{\overset{\gamma}{\rightleftharpoons}} \emptyset, \qquad \mathrm{y}_i \xrightarrow{\gamma} \emptyset, \qquad \mathrm{C}_i \xrightarrow{\gamma} \emptyset,$$

where a_i and d_i represent the binding and unbinding rate constants of the resource with the DNA, and k_i represents the rate of protein production. Using the law of mass action [5], the set of ODEs describing the dynamics of this system are given by

$$\dot{R} = \alpha - \gamma R + \underbrace{\sum_{i=1}^{n} \boxed{(d_i + k_i)C_i - a_i D_i R}}_{s} \tag{10a}$$

$$\dot{C}_i = a_i D_i R - (d_i + k_i + \gamma)C_i \tag{10b}$$

$$\dot{y}_i = k_i C_i - \gamma y_i, \tag{10c}$$

where α is the rate of production of the resources and γ is the dilution of all species due to cell growth. Referring to Fig. 5, s in (10a) is the retroactivity applied to the resource module by all its downstream modules. Note that since the terms in the red box are summed in (10a) to obtain s, the retroactivity to the resource module behaves in series as shown in Fig. 5. The retroactivity to the resource module affects the availability of resources to all modules in the system, which may affect the system's overall function, as we illustrate next.

The system of equations (10) may be reduced by taking into account that the binding and unbinding of D_i with R occurs much faster than the other processes, so timescale separation may be used [5]. Additionally, since we are interested in the behavior of the modules (transmission paths 1 and 2) and not in the specific effects of retroactivity on the resource module, we can reduce the set of ODEs (10) by replacing the ODE for R in (10a) with the algebraic conservation law [5] given by

$$R_{tot} = R + \sum_{j=1}^{n} C_j, \tag{11}$$

where R_{tot} is the total concentration of the resource given by α/γ. Now, since the rate of binding and unbinding is much faster than the dynamics of the other proteins, we find the quasi-steady state of C_j as

$$\overline{C}_j = R\frac{D_j}{K_j}, \tag{12}$$

where $K_j = \frac{a_j}{d_j + k_j + \gamma}$ is the effective binding constant of DNA with the resource. Substituting (12) into (11) for each $\overline{C}_j$, we solve for the free concentration of resources as

$$R = \frac{R_{tot}}{1 + \sum_{j=1}^{n} \frac{D_j}{K_j}}. \tag{13}$$

Thus, the availability of free resources depends on the DNA, D_j, from each module. In turn, the effective rate of production $k_i C_i$ of the module's output y_i given in (10c) depends on the availability of free resources given in (13). Therefore, the rate of production of gene expression–the method of information processing–in every module depends on every other module in the network. This may be generalized to include external inputs and connections between modules such as in the sender/receiver configuration in Fig. 5, which gives the general module output dynamics as

$$\dot{y}_i = \frac{\overbrace{F_i(\mathbf{u}, \mathbf{y})}^{g_i(\mathbf{u},\mathbf{y})}}{1 + \boxed{\sum_{k=1}^{n} J_k F_k(\mathbf{u}, \mathbf{y})}} - \gamma y_i \tag{14}$$

as derived in [64] and experimentally verified in [26]. Here F_i is the intended regulatory function and, for example, may be given by either (3) or (4) for each module i, $\mathbf{y}$ is the set of all outputs of the modules in the system, $\mathbf{u}$ is the set of external inputs to the system, and J_k is the resource demand coefficient for each module. The resource sharing term is defined as $R(\mathbf{u}, \mathbf{y}) = \sum_{k=1}^{n} J_k F_k(\mathbf{u}, \mathbf{y})$, boxed in red in (14).

From (14), and shown in detail in [26, 64], 'hidden' indirect interactions appear among the system's modules due to retroactivity to the resource module. Specifically, as the output of one module increases (increasing the value of $R(\mathbf{u}, \mathbf{y})$), this decreases the available quantity of resources to other modules through sequestration of the resource. This decrease in availability of resources slows the rate of protein production of all other modules which decreases the output of each module. This effect is demonstrated in Fig. 6 where two unconnected modules, depicted as nodes, are shown. As the input to y_1 is increased, the output of y_2 decreases since y_1 sequesters the available resources, leaving less for y_2. This has been shown to cause more than a 60% decrease in the output of any node experimentally in bacterial circuits [27].

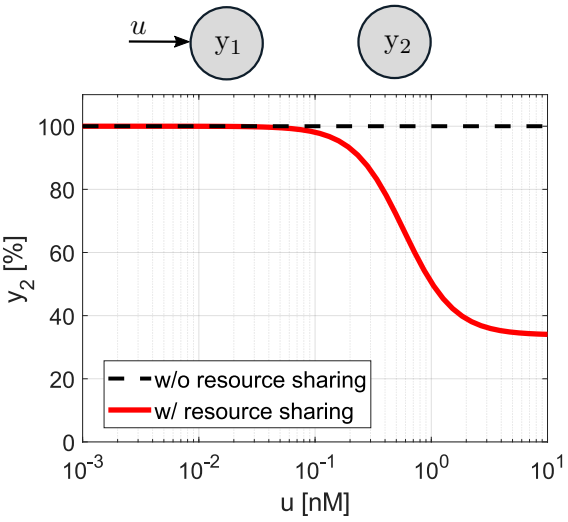

Fig. 6. Changes in one node affect other nodes due to resource sharing even if the nodes are not connected through regulatory links. As the input to the first node is increased, the output of the second node decreases (red) compared to the expected output if there were no resource sharing between the two nodes (black). The output y_2 is normalized as a percentage of its concentration without resource sharing. Details regarding the equations and parameters used in this simulation are given in Appendix A.

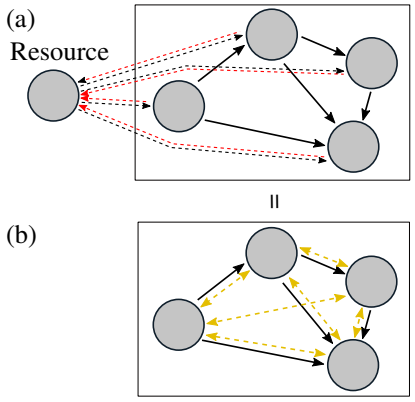

Fig. 7. Hidden interactions due to resource sharing. (a) The cellular resource is an input to all nodes in the network. Due to retroactivity between the resource and the other nodes (red arrows), the availability of the resource depends on all nodes in the network. Retroactivity arrows between node within the module not shown. (b) When the dynamics of the resource are replaced with its conservation law, a hidden interaction network due to interactions between each node and the resource arises (yellow arrows).

B. Effect of Resource Sharing on a Network

The consequences of these hidden interactions can be formally captured by constructing the hidden interaction graph [64] (Fig. 7). Specifically, given an intended regulatory network as illustrated in the box in Fig. 7a, and accounting for the fact that the interactions with the resource node are fast compared to the dynamics of the network (from Section IVA), we obtain an equivalent network, whose graph is given by the superposition of intended regulatory interactions and hidden interactions (Fig. 7b).

We now describe how a network graph of a genetic circuit with resource sharing may be drawn given the ODE model of the system. We create a signed, weighted, directed graph using the Jacobian matrix of (14) as follows. The intended regulatory interaction graph is determined by the function $F_i(\mathbf{u},\mathbf{y})$. Specifically, considering (14), an edge is drawn from node y_j to y_i according to $\operatorname{sign}\left(\frac{\partial F_i}{\partial y_j}\right)$: if $\operatorname{sign}\left(\frac{\partial F_i}{\partial y_j}\right) > 0$, the edge is positive from y_j to y_i (activation, represented by "$\rightarrow$"), and if $\operatorname{sign}\left(\frac{\partial F_i}{\partial y_j}\right) < 0$, the edge is negative (repression, represented by "$\dashv$").

Due to resource sharing, 'hidden' interactions arise, creating a hidden interaction graph. The hidden interaction graph is determined by $\operatorname{sign}\left(\frac{\partial R(\mathbf{u},\mathbf{y})}{\partial y_j}\right)$, which arises due to unintended interactions from resource sharing effects. Specifically, since $R(\mathbf{u},\mathbf{y})$ appears in the denominator of (14), a positive edge is drawn from y_j to all other nodes if $\operatorname{sign}\left(\frac{\partial R(\mathbf{u},\mathbf{y})}{\partial y_j}\right) < 0$, and a negative edge is drawn from y_j to all other nodes if $\operatorname{sign}\left(\frac{\partial R(\mathbf{u},\mathbf{y})}{\partial y_j}\right) > 0$. Since $R(\mathbf{u},\mathbf{y})$ depends on all nodes in the network, the hidden interaction graph is a complete graph. The effective interaction graph is determined by the sum of the intended regulatory interaction graph and the hidden interaction graph, and may be computed using $\operatorname{sign}\left(\frac{\partial g_i}{\partial y_j}\right)$ [65].

Graphical rules for drawing the effective interactions are given in Fig. 8. In general, the hidden interactions have the effect of decreasing the strength of effective interactions throughout the network by making positive interactions less positive (or possibly negative), and negative interactions less negative (or possibly positive). Specifically, for an upstream node with only one downstream node, the hidden interactions do not change the sign of the intended regulatory interaction, but they weaken it (Fig. 8a). Additionally, as one node is activated, it sequesters more resources, leaving less for other nodes. Therefore, this creates a hidden repression on all other nodes (Fig. 8b). The situation is similar for repression, which creates hidden activations. Finally, if an upstream node has multiple downstream nodes, the effective interactions may be either positive or negative, depending on the specific parameters and the rest of the network (Fig. 8c).

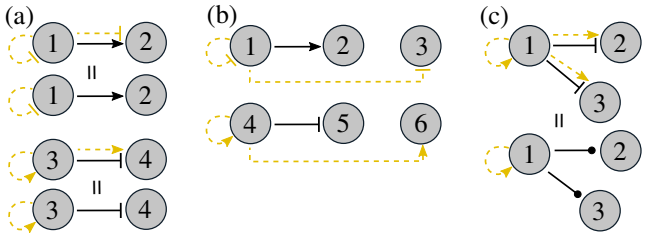

Fig. 8. Rules for drawing hidden and effective interactions. (a) For a system consisting of only two nodes with activation (black arrows) between them (node 1 activates node 2), the hidden interactions (yellow arrows) are repression from the upstream node (node 1) to itself and the downstream node (node 2), but the superposition of the hidden and intended interaction remains activation. For a two-node system with repression between them (nodes 3 and 4), the hidden interactions are activation, similarly, but the superposition of the hidden and intended interaction remains repression. (b) For three nodes with one intended activation (node 1 activates node 2), the hidden interactions are repression from the upstream node (node 1) to all other nodes (nodes 2 and 3). For three nodes with one intended repression (node 4 represses node 5), the hidden interactions are activation from the upstream node (node 4) to all other nodes (nodes 5 and 6). (c) For nodes with multiple downstream targets (node 1), the effective interactions are undetermined and may be either positive or negative, depending on the specific parameters and the rest of the network. When the strength of one of the repressive arrows is much stronger than the other, the change due to resource sharing effects on the other, may be stronger than the TX regulation effect, resulting in a possible sign change due to resource sharing.

Now, we review some experimental results demonstrating the effects of resource sharing in genetic circuits. In [66], the authors have shown parallels between the steady state of a network with resource sharing and Ohm's law of a circuit with resistors in series. As nodes are added to the network, the system acts as a voltage divider with the output of each node being proportional to the resource usage divided by the total resource usage of the circuit. Gyorgy et. al considered a network with two unconnected nodes and demonstrated that as the input of one node is changed, the output of the other node changes by more than 60% [27]. Specifically, the authors show that as the input of the first node is increased, the output of the second node decreases and approximately follows a line in the x_1–x_2 plane where x_1 and x_2 are the concentrations of the proteins in the two nodes. From this, they derive fundamental limitations on the realizable region of the possible outputs for any network [67]. In [26], the authors demonstrate that resource sharing effects may cause unexpected, destructive behavior of circuit components. They consider a three-node activation cascade where every pair of

interactions is activation. This circuit should give an increasing input-output response curve; however, they observe that the actual behavior is such that the output decreases as the input to the cascade is increased. This unexpected behavior is due to resource sharing effects where the middle node in the cascade imparts a large retroactivity flux to the resources, leaving few available resources for the output node to function. This demonstrates that the expected behavior of even simple systems may be destroyed due to resource sharing. As genetic networks become larger and more complex, resource sharing is an increasingly important aspect to consider in design of circuits to build larger, more sophisticated networks.

V. Modular Composition in the Face of Retroactivity

The previous section described the causes and effects of retroactivity and its implications in a resource sharing context. This section describes the tools developed in order to allow predictable composition of systems, despite the presence of retroactivity.

Modular composition of subsystems to form larger, more complex circuits is central to design in many engineering disciplines. However, modules connected to others rarely behave as they did in isolation. In electrical circuits, impedance effects are one of the chief causes of this lack of modularity. Several tools have been developed to help characterize the behavior of connected modules by considering appropriate descriptions in isolation. One such tool is Thévenin's theorem (and its dual, Norton's theorem), which states that any electrical circuit can be replaced by an equivalent circuit consisting of a voltage source (current source in the case of Norton) and an impedance [68–70]. This allows one to easily predict the output voltage of an electrical network once it has been connected to another (possibly complex) electrical network (Fig. 9).

In [60], Gyorgy and Del Vecchio provide a theorem for gene transcription networks conceptually analogous to Thévenin's. This theorem allows for the determination of the dynamics of connected modules by considering their models in isolation, shown in Fig. 10. The system in this figure is composed of module A, which has state x^A, takes input u^A, and has an output y^A, with dynamics $\dot{x}^A = f_0^A(x^A, u^A)$ in isolation. This module is connected to downstream module B, with state x^B, which takes the output y^A of module A as input and has dynamics $\dot{x}^B = f_0^B(x^B, y^A)$. Then, the following sources of retroactivity affect the isolated dynamics of these modules, as shown in Fig. 10. Internal retroactivity R arises for modules composed of more than one node, where "child" nodes impart a signal to "parent" nodes due to retroactivity, shown by the pink arrow in Fig. 10. Scaling and mixing retroactivity arise when modules are interconnected, and are shown by the magenta and yellow arrows, respectively, in Fig. 10. Denoting the internal retroactivity matrix of module A by R^A, and S^B and M^B as the scaling and mixing retroactivity matrices, respectively, of module B, the modified dynamics of module A can be written as

$$\begin{aligned}\dot{x}^A =&(I + (I + R^A)^{-1}S^B)^{-1} f_0^A(x^A, u^A) \\ &- (I + (I + R^A)^{-1}S^B)^{-1}(I + R^A)^{-1} M^B f_0^B(x^B, y^A).\end{aligned} \tag{15}$$

Scaling retroactivity S^B (magenta arrow in Fig. 10) is imparted to the module A by module B due to the reversible binding of the output of module A to its target in module B. It is so named because it adds a scaling term to the dynamics of module A, as seen in (15). When a target node of module A in module B also has a parent node in module B, this parent node can affect the retroactivity flux to the output of module A. This occurs, for example, if the output protein of the parent node competes with the output protein of module A to bind to the target. This is called mixing retroactivity M^B (yellow arrow in Fig. 10), so named because it adds (mixes) the dynamics of the downstream module to the dynamics of the upstream module, as seen in (15).

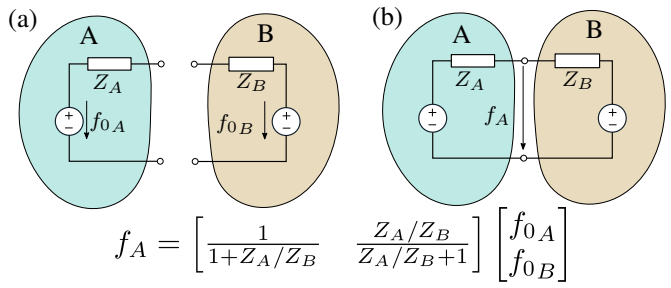

Fig. 9. Demonstration of Thévenin's theorem for electrical circuits. (a) An electrical circuit module may be replaced with an equivalent voltage source and impedance. The voltage across both modules in isolation are f_{0A} and f_{0B}. (b) When two circuit modules are connected, the voltage across the connected modules changes compared to that of the modules in isolation according to the impedances Z_A and Z_B as in the equation.

The work by Gyorgy and Del Vecchio gives explicit formulae for these matrices in terms of the reaction-rate coefficients of gene regulatory modules and the network interaction graph. For example, consider a system with one upstream node x_1, with promoter concentration D_1, that undergoes negative autoregulation. The isolated ODE for the dynamics of x_1, ignoring the retroactivity due to the load of its own promoter, is written in the form of (4), specifically, $\dot{x}_1 = f(x_1) = \frac{\beta}{1+x_1^n} - \gamma x_1$. Now, suppose that this node is connected to downstream sites with promoter concentration D_2 such that x_1 activates these sites. Upon interconnection and considering the effect of internal retroactivity, the dynamics of x_1 change to become

$$\dot{x}_1 = \frac{1 + R(x_1)}{1 + R(x_1) + S(x_1)} f(x_1),$$

where $R(x_1) = D_1 \frac{n^2 x_1^{n-1}}{k_1} \left(1 + \frac{x_1^n}{k_1}\right)^{-2}$ is the internal retroactivity due to the binding of x_1 with its own promoters for autoregulation and k_1 is the dissociation constant of this binding. $S(x_1) = D_2 \frac{n^2 x_1^{n-1}}{k_1} \left(1 + \frac{x_1^n}{k_1}\right)^{-2}$ is the scaling retroactivity due to the binding of x_1 to the downstream promoters. Note that increasing the internal retroactivity for a system makes it more robust to interconnections, at the expense of response speed. Such a characterization of retroactivity, in terms of R, M, and S, for each module allows for the determination of the module's behavior when connected to another module described by (15).

Other works that assist in modular circuit design in the presence of retroactivity are [71–73]. Similar to the concept of

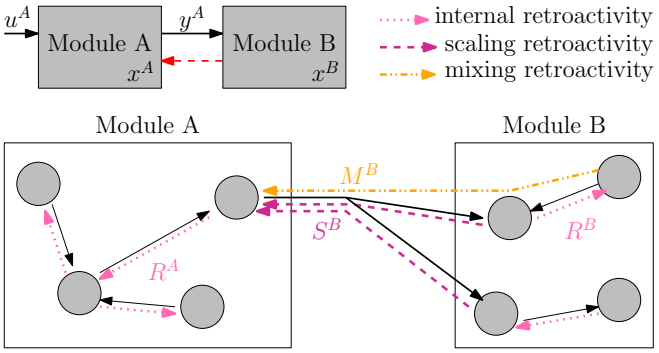

Fig. 10. Internal, scaling and mixing retroactivity. Module A, with state x^A, input u^A and output y^A is connected to downstream module B with state x^B. Internal retroactivity (R^A, R^B) of a module is the effect of the retroactivity signals among nodes within the same module. Scaling and mixing retroactivities S^B and M^B are the effects of the retroactivity signals from nodes in the downstream module B onto nodes of the upstream module A.

fan out in electrical circuits (the number of logic gate inputs a given logic gate output can drive), fan out is defined for gene regulatory networks [71, 72] as "a measure of the maximum number of promoter sites that the output transcription factors of the upstream module can regulate without significant slowdown in the kinetics of the output", and an experimental method to estimate fan-out is proposed. Fan out thus provides a method to quantify the robustness of an upstream system to a downstream load.

In the specific case of genetic circuits with resource sharing, the problem of modular composition has been addressed in [74], where metrics were introduced for quantifying resource sharing: Q, the quantity of resources used by a module, and S', the sensitivity of the output of the module to disturbances in the availability of resources. By appending information of Q and S' to a module's description characterized in isolation, we can predict the steady state behavior of any module i when its context changes due to the presence of other modules. Specifically, let y_i be the steady state output of the module of interest (module i) in isolation, and let S'_j and Q_j be the resource sharing metrics for any module j. Then the relative change in the output of module i with respect to the output of the module in isolation is given by the product of the sensitivity of module i (S'_i) with the total resource sharing disturbance from the other modules ($\sum_{j\neq i} Q_j$), i.e. $\frac{y_i^*-y_i}{y_i} = S'_i \sum_{j\neq i} Q_j$ where y_i^* is the output of the module when perturbed. This may be solved to give the steady state output y_i^* when module i shares resources with other modules ($j \neq i$) as

$$y_i^* = y_i \left(1 + S'_i \sum_{j\neq i} Q_j\right). \tag{16}$$

This allows us to replace any collection of nodes in a circuit with a black box that has the same input-output behavior in isolation and particular values of Q and S'. Then, it is guaranteed that the input-output behavior of the system when composed with other circuits is predicted by (16), which is conceptually similar to Thévenin's theorem in electrical circuits (Fig. 9). The authors additionally show that the metrics Q and S' may be measured through a systematic experimental procedure. These metrics allow for the prediction of the behavior of genetic circuits when composed with other modules that share the same resource pool. For example, suppose one module has a large Q, and another has a large S'. If they are placed in the same cell, then it is likely that the latter module will not behave as it did when tested without the presence of the first module.

VI. Using Feedback Control to Attenuate Retroactivity and Enforce Circuit Modularity

One approach to handle retroactivity during circuit design is to engineer circuit modules such that their input-output behavior is robust to retroactivity, effectively enforcing modularity by design. In this case, one can compose modules safely assuming that their input-output behavior stays unchanged upon composition. Feedback control in electrical circuits has been pivotal in achieving effectively modular behavior in the face of disturbances thus allowing a designer to "forget" about the complexities within each module and to regard each module as a simple input-output transfer function. In the case of biomolecular circuits, retroactivity arising from loads and perturbations in resource availability can be viewed as disturbances. This section describes the use of feedback control to attenuate the effects of these disturbances on a circuit's function, effectively enforcing unidirectional signal transmission.

A. Insulation Devices: Enforcing Unidirectional Signal Transmission in Biomolecular Networks

Consider the system in Fig. 11a, where module 1 (sender) is connected to module 2 (receiver). The problem of connecting these modules without having the transmitted information u be affected by retroactivity, s, can be addressed by placing an *insulation device* between these two modules. An insulation device is a system that, when connected between an upstream sender and a downstream receiver, imparts a low retroactivity to the input (i.e., $r \approx 0$) and attenuates the effect of the retroactivity to the output s on y [22], therefore allowing unidirectional transmission of information (from upstream module 1 to downstream module 2). The retroactivity signal, s, can be treated as a disturbance acting on the insulation device, and, drawing from solutions in classical controls for disturbance attenuation [52], high-gain feedback can be used to attenuate s. This concept is illustrated in Fig. 11b, where G is a large gain that multiplies the error, $\bar{u} - Ky$, between the reference input $\bar{u}$ and a scaled (by K) version of the output y, which is affected by the disturbance s. This block diagram leads to

$$y = G(\bar{u} - Ky) + s,$$

which can be rearranged as

$$y = \frac{G}{1+KG}\bar{u} + \frac{s}{1+KG}.$$

Then, as G grows, the output y tends to $\frac{\bar{u}}{K}$, which is independent of the retroactivity signal s, thus achieving retroactivity attenuation.

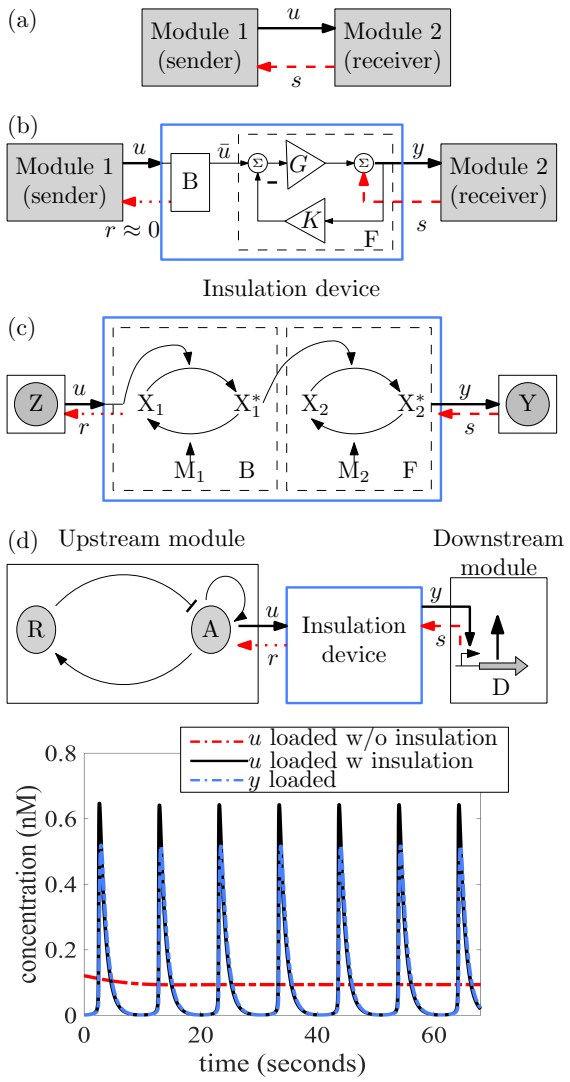

Fig. 11. Concept and biological realization of an insulation device. (a) Module 1 is subject to retroactivity (red arrow) when directly connected to Module 2. (b) An insulation device consisting of a buffer stage B that imparts a small retroactivity r to its input, and a high-gain (G) negative feedback (K) stage F that attenuates the effect of the retroactivity signal s on its output. (c) A biomolecular realization of an insulation device consisting of a two-stage phosphorylation cycle cascade, where the first cycle plays the role of the buffer system B by having a low concentration of X_1 and the second cycle attenuates retroactivity to the output through high-gain feedback - achieved by a high concentration of X_2 and M_2 [29, 75]. (d) The two-stage phosphorylation cycle based insulation device is connected between the clock of Fig. 2 and its downstream system. In the presence of the insulation device, the oscillations of the clock are restored (black plot) and faithfully transmitted to the downstream module (blue dash-dotted plot). Details regarding the equations and parameters used in the simulations are given in Appendix C.

Insulation devices that use this general mechanism for attenuation of the retroactivity to the output s have been designed and implemented through appropriate biomolecular processes [22, 29, 32, 75–79]. Signaling circuits, such as phosphorylation and phosphotransfer cycles, consist of two processes: one process that upregulates the output, (such as phosphorylation) and one process that downregulates the output (such as dephosphorylation). These processes form a cycle that can act as a high-gain negative feedback system where the high gain, G, can be achieved by increasing together the total substrate and phosphatase concentrations, X_T and M_T, and the negative feedback factor, K, can be tuned by changing the ratio of the substrate to the phosphatase $\frac{X_T}{M_T}$ [22]. In such a way, one-stage signaling cycles have been shown to use high-gain negative feedback to attenuate the effects of the retroactivity to the output, s, both theoretically [22, 77], and through *in vivo* experiments in bacterial circuits [32]. However, the devices built with a single stage signaling cycle show a design trade-off where the high-gain feedback design (while attenuating s) leads to a high retroactivity to the input, r, due to the large substrate concentration [22, 32, 77, 78].

In [79], it was shown that a cascade of signaling cycle stages (such as the one shown in Fig. 11c) can overcome the aforementioned trade-off, where the last cycle attenuates the effects of the retroactivity to the output s through high-gain feedback, and the first cycle imparts a low retroactivity to input, r. Thus, an insulation device designed where the first stage is a cycle with low substrate concentration (buffer stage B), and the second and last stage is a cycle with high substrate concentration (high-gain negative feedback stage F), can impart a low retroactivity to the input, r, and attenuate the effects of the retroactivity to the output, s, as shown in Fig. 11c. Such a two-stage insulation device was built *in vivo* in eukaryotic cells in [29] and was shown to completely restore the performance of the circuit in the presence of load.

We illustrate the operation of this insulation device in Fig. 11d, in which it is used between the clock of Fig. 2 and its downstream system. Simulations in Fig. 11d show that, due to the low retroactivity to the input, r, the oscillations of the clock are restored (black line), and due to the attenuation of the retroactivity to the output, s, these oscillations are transmitted faithfully to the downstream load (blue dash-dotted line).

In [75], an analytical framework was provided for evaluating the ability of natural signaling circuits to act as insulation devices. This framework was applied to evaluate frequently occurring signaling cycle cascades to develop a library of well-characterized insulation devices.

B. Decentralized Feedback Control: Attenuation of Effects of Hidden Interactions due to Resource Sharing

We now wish to decrease the effects of the hidden interactions due to resource sharing (Fig. 7) and recover the intended interaction graph of the network. At a high level, we seek to design a local feedback controller within each node of the network such that, with this feedback in place, the hidden interactions have little or no effect on the network's behavior, leaving only the network created by the intended regulatory interactions (Fig. 12).

Specifically, by focusing on the signals that pass through each node, we have the situation in Fig. 13a [30, 65]. Each node may be considered as a two-input two-output system that takes a reference signal, u_i, and a disturbance signal, w_i, as input and gives an output, y_i, and a disturbance output, d_i, due to the perturbation on the availability of resources. Thus, we wish to design a feedback controller around each node to decouple it from the disturbances (Fig. 13b). The problem of making an output of interest y_i dependent only on a reference

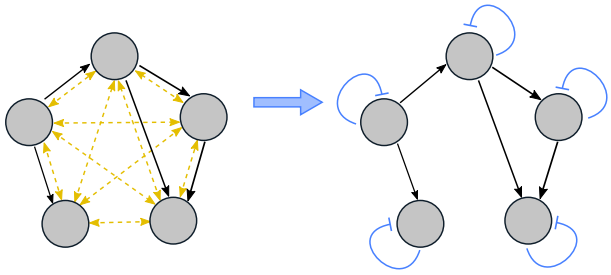

Fig. 12. Decentralized feedback control to attenuate hidden interactions due to resource sharing. The goal of decentralized feedback control in genetic networks to attenuate resource sharing is to recover the intended interactions graph (black arrows) while attenuating the unintended hidden interactions due to resource sharing (yellow dashed arrows). By implementing a negative feedback controller at each node, it is possible to decouple the intended interactions and the hidden interactions.

input while making it independent of a disturbance input, w_i, is a classical disturbance attenuation problem [52].

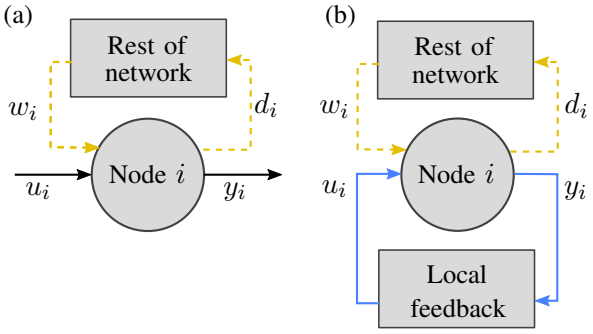

Fig. 13. Local feedback controller to decouple node behavior from hidden interactions (yellow arrows). (a) A node in a genetic network where an input disturbance w_i comes from perturbations in the availability of resources imparted by the rest of the network and the output disturbance d_i contributes to these perturbations to the rest of the network. The intended input is u_i and output is y_i. (b) We wish to design a local control system around each node to decouple the input-output behavior of the node from the undesired interactions.

To solve the problem of network disturbance decoupling, we must solve two sub-problems. First, if we assume that w_i does not come from the network, we need to solve a standard disturbance attenuation problem. Second, assuming we have solved this problem, we must guarantee that the network with these feedback controllers in place remains stable. In fact, referring to Fig. 13b, due to the loop created by the hidden, yellow interactions between the input disturbance w_i and output disturbance d_i, the network may lose stability in the presence of the local feedback controllers. Specifically, when a controller is implemented around each node as in Fig. 13b, the output disturbance d_i may become amplified with respect to the input disturbance w_i. Since the output disturbance d_i then affects other nodes in the network as their input disturbance, this may cause the disturbance signals to grow indefinitely, leading to the system's instability. Therefore, we must also solve a second problem of network stability to guarantee that the local disturbance attenuation is globally successful.

First, to solve the local disturbance attenuation problem, a feedback controller can be used to attenuate the effect of the resource disturbance at each node. This controller may be implemented through sRNA-enabled silencing of mRNA [30, 33]. In related works, this negative feedback control scheme has been called an anthitetic feedback controller [31, 80]. An sRNA is a species that is found in bacterial cells, which binds to a complementary mRNA and degrades it rapidly [81]. Since the sRNA does not use ribosomes in its production, it is not affected by the disturbance due to resource sharing, which is dominated by the limitations in the pool of ribosomes [27]. Specifically, it was theoretically shown that sRNA-mediated negative feedback on each node changes the node dynamics to create a quasi-integral controller [82]. This quasi-integral controller rejects disturbances asymptotically as the gain, G, of the controller becomes large. The gain of the controller, G, physically corresponds to the lumped rate of degradation of mRNA via sRNA, so that when the mRNA degrades very quickly, G is large.

To solve the second problem of network stability, we can apply a line of reasoning similar to that of the small gain theorem for networks [83] as follows. Here, we explain the qualitative reasoning, and our arguments are not mathematically rigorous. For a detailed mathematical treatment, the reader is referred to [30, 65]. Referring to Fig. 13b, let the steady-state input-output map for the output disturbance, d_i, of node i as the feedback gain G becomes large be

$$\lim_{G\to\infty} d_i(u_i, w_i, G) = g_i(u_i) + \hat{g}_i(u_i)w_i, \tag{17}$$

and let $w_i = \sum_{j\neq i} d_i$. Then the disturbance interconnection matrix is

$$A_{ij} = \begin{cases} 1 & \text{if } i = j \\ -\hat{g}_j(u_j) & \text{if } i \neq j, \end{cases} \tag{18}$$

which describes the interactions of the nodes through the disturbances d_i and is found by substituting $w_i = \sum_{j\neq i} d_i$ in (17) and solving for every d_i as $G \to \infty$. If A_{ij} is diagonally dominant, i.e., the sum of the elements of A in each row is less than the magnitude of the element on the diagonal, then the network is guaranteed not to amplify the steady state signals through the yellow, hidden interactions (Fig. 13b) after implementing feedback [30, 65]. Qualitatively, if the total sum of disturbances to the network $\hat{g}_i(u_i)$ is small enough such that the disturbance signal, d_i, of each node becomes "smaller" than the input disturbance, w_i, then the network is guaranteed to have a bounded steady state solution. We note that this result applies only to steady state behavior, and its extension to dynamic behavior and system stability is still a subject of investigation.

In Fig. 14, we revisit the illustrative example in Fig. 6 and show that the local feedback controller attenuates the disturbance due to resource sharing for different values of the feedback gain, G. Again, we consider a system of two unconnected nodes y_1 and y_2, where y_1 has an external input u. As the value of the input u is changed, we observe the effect on the steady state of y_2. Comparing the systems without feedback (Fig. 14a) to the systems with feedback (Fig. 14b), the effect of the resource disturbance on the steady state of y_2 is attenuated when the local feedback controller is added.

Along these lines, a variety of controller designs have been proposed and shown to achieve the goal of attenuating

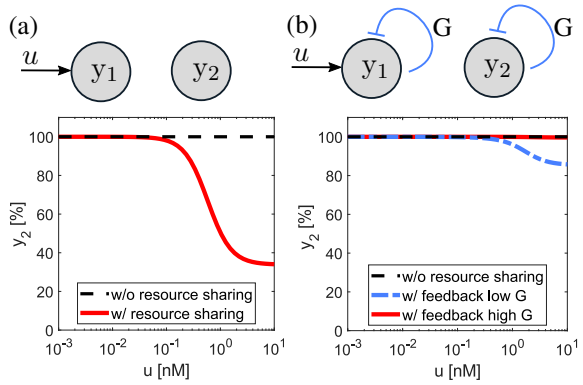

Fig. 14. The effect of the local feedback on decoupling resource disturbances in a two-node system. (a) The steady state response for the system without local feedback. Due to resource sharing the output of y_2 with resource sharing (red line) is decreased by more than 60% compared to the system without resource sharing (black dashed line) as the input to y_1 is increased. (b) The steady state response for the system with local feedback for different values of feedback gain, G, compared to the system without resource sharing (black dashed line). The low gain case is with $G = 1$ (blue dash-dot line) and high gain case is with $G = 10$ (red line). The effect of resource sharing on the steady state of y_2 due to resource sharing is decreased through the use of the feedback compared to without feedback and improves with higher gain. Details regarding the equations and parameters used in this simulation are given in Appendix A and B.

disturbance due to resource sharing. This includes the creation of decentralized high-gain negative feedback quasi-integral controllers in genetic circuits [31, 33, 65, 80, 82, 84, 85]. These controllers are robust, that is, they can decouple the network, independent of the specific parameters of each node. This is especially beneficial in genetic networks where the dynamics of each node are highly uncertain. An orthogonal line of work considers attenuating the retroactivity s in Fig. 5 through a centralized feedback controller on the resource module [86].

VII. Conclusions

Modularity of functional components plays a crucial role in the bottom-up design of synthetic biomolecular circuits. This review has focused on two main causes of loss of modularity: loads due to direct connectivity, and indirect connectivity arising from loads applied to shared cellular resources. We reviewed the concept of retroactivity, which was introduced to capture the problem of loads within a formal signals and systems formulation, making the load problem amenable to mathematical study and engineering solutions. Specifically, we summarized the theoretical developments and the experimental validation for the characterization of retroactivity effects, and reviewed engineering solutions that aim to make biomolecular circuits modular. Motivated by the success of feedback control in aiding modular design in traditional engineering disciplines, feedback control has been used to overcome effects of retroactivity. This has been performed through the design of insulation devices to attenuate the effects of loads due to direct connectivity, and through the design of decentralized feedback controllers to overcome effects of indirect connectivity due to resource sharing. Although these solutions broadly use standard problem formulations from control theory, the solutions to these problems are often non-standard and require the development of new theory due to the unique nature of the physical processes that transmit information in biomolecular systems.

Although much progress has been made on this front, a number of remarkable challenges still exist to make modular design practically possible. Many of these challenges fall within the fields of communications, signal processing, dynamical systems, and feedback control as they require a deeper understanding of the dynamical interactions among processes that transmit and receive information [21, 87]. Major issues include noise and stochastic behavior, parameter uncertainty, fragility to perturbations in environmental conditions, and unwanted interactions with endogenous circuitry components. It is likely that the merging of a number of well-established fields including control theory, signal processing, communications, dynamical systems, and stochastic processes will be required to address these problems.

References

[1] J. López-Barneo, R. Pardal, and P. Ortega-Sáenz, "Cellular mechanism of oxygen sensing," *Annual review of physiology*, vol. 63, no. 1, pp. 259–287, 2001.

[2] E. A. Veal, A. M. Day, and B. A. Morgan, "Hydrogen peroxide sensing and signaling," *Molecular cell*, vol. 26, no. 1, pp. 1–14, 2007.

[3] A. P. Gasch, P. T. Spellman, C. M. Kao, O. Carmel-Harel, M. B. Eisen, G. Storz, D. Botstein, and P. O. Brown, "Genomic expression programs in the response of yeast cells to environmental changes," *Molecular biology of the cell*, vol. 11, no. 12, pp. 4241–4257, 2000.

[4] H. L. Bradlow, *Signal transduction and communication in cancer cells*, vol. 1028. New York Academy of Sciences, 2004.

[5] D. Del Vecchio and R. M. Murray, *Biomolecular Feedback Systems*. Princeton: Princeton University Press, Oct. 2014.

[6] M. Ptashne, *A genetic switch: Gene control and phage lambda*. Cell Press and Blackwell Scientific Publications, Jan. 1986.

[7] S. Huang, Y.-P. Guo, G. May, and T. Enver, "Bifurcation dynamics in lineage-commitment in bipotent progenitor cells," *Developmental Biology*, vol. 305, pp. 695–713, May 2007.

[8] L.-C. Fortier and O. Sekulovic, "Importance of prophages to evolution and virulence of bacterial pathogens," *Virulence*, vol. 4, pp. 354–365, July 2013.

[9] Y. Qian, C. McBride, and D. D. Vecchio, "Programming cells to work for us," *Annual Review of Control, Robotics, and Autonomous Systems*, vol. 1, no. 1, p. null, 2018.

[10] T. S. Gardner, C. R. Cantor, and J. J. Collins, "Construction of a genetic toggle switch in Escherichia coli," *Nature*, vol. 403, pp. 339–342, Jan. 2000.

[11] M. B. Elowitz and S. Leibler, "A synthetic oscillatory network of transcriptional regulators," *Nature*, vol. 403, pp. 335–338, Jan. 2000.

[12] M. O. Din, T. Danino, A. Prindle, M. Skalak, J. Selimkhanov, K. Allen, E. Julio, E. Atolia, L. S. Tsimring, S. N. Bhatia, and J. Hasty, "Synchronized cycles of bacterial lysis for *in vivo* delivery," *Nature*, vol. 536, pp. 81–85, Aug. 2016.

[13] D. Chakravarti and W. W. Wong, "Synthetic biology in cell-based cancer immunotherapy," *Trends Biotechnol.*, vol. 33, pp. 449–461, Aug. 2015.

[14] A. Prindle, P. Samayoa, I. Razinkov, T. Danino, L. S. Tsimring, and J. Hasty, "A sensing array of radically coupled genetic 'biopixels'," *Nature*, vol. 481, pp. 39–44, Jan. 2012.

[15] P. P. Peralta-Yahya, F. Zhang, S. B. d. Cardayre, and J. D. Keasling, "Microbial engineering for the production of advanced biofuels," *Nature*, vol. 488, pp. 320–328, Aug. 2012.

[16] F. Zhang, J. M. Carothers, and J. D. Keasling, "Design of a dynamic sensor-regulator system for production of chemicals and fuels derived from fatty acids," *Nature Biotechnology*, vol. 30, pp. 354–359, Apr. 2012.

[17] D. E. Cameron, C. J. Bashor, and J. J. Collins, "A brief history of synthetic biology," *Nat Rev Micro*, vol. 12, pp. 381–390, May 2014.

[18] P. E. M. Purnick and R. Weiss, "The second wave of synthetic biology: from modules to systems," *Nat Rev Mol Cell Biol*, vol. 10, pp. 410–422, June 2009.

[19] C. T. Y. Chan, J. W. Lee, D. E. Cameron, C. J. Bashor, and J. J. Collins, "'Deadman' and 'Passcode' microbial kill switches for bacterial containment," *Nat Chem Biol*, vol. 12, pp. 82–86, Feb. 2016.

[20] M. N. Win and C. D. Smolke, "Higher-order cellular information processing with synthetic RNA devices," *Science*, vol. 322, pp. 456–460, Oct. 2008.

[21] D. Del Vecchio, "Modularity, context-dependence, and insulation in engineered biological circuits," *Trends Biotechnol.*, vol. 33, pp. 111–119, Feb. 2015.

[22] D. Del Vecchio, A. J. Ninfa, and E. D. Sontag, "Modular cell biology: retroactivity and insulation," *Molecular Systems Biology*, vol. 4, no. 1, p. 161, 2008.

[23] S. Jayanthi, K. S. Nilgiriwala, and D. Del Vecchio, "Retroactivity controls the temporal dynamics of gene transcription," *ACS synthetic biology*, vol. 2, no. 8, pp. 431–441, 2013.

[24] P. Jiang, A. C. Ventura, E. D. Sontag, S. D. Merajver, A. J. Ninfa, and D. Del Vecchio, "Load-induced modulation of signal transduction networks," *Sci. Signal.*, vol. 4, no. 194, pp. ra67–ra67, 2011.

[25] A. C. Ventura, P. Jiang, L. Van Wassenhove, D. Del Vecchio, S. D. Merajver, and A. J. Ninfa, "Signaling properties of a covalent modification cycle are altered by a downstream target," *Proceedings of the National Academy of Sciences*, vol. 107, no. 22, pp. 10032–10037, 2010.

[26] Y. Qian, H.-H. Huang, J. I. Jiménez, and D. Del Vecchio, "Resource competition shapes the response of genetic circuits," *ACS Synth. Biol.*, vol. 6, pp. 1263–1272, July 2017.

[27] A. Gyorgy, J. I. Jiménez, J. Yazbek, H.-H. Huang, H. Chung, R. Weiss, and D. Del Vecchio, "Isocost lines describe the cellular economy of genetic circuits," *Biophysical Journal*, vol. 109, pp. 639–646, Aug. 2015.

[28] D. L. Schilling and C. Belove, *Electronic Circuits: Discrete and Integrated*. McGraw-Hill Education, 1968. Google-Books-ID: 4RojAAAAMAAJ.

[29] D. Mishra, P. M. Rivera, A. Lin, D. Del Vecchio, and R. Weiss, "A load driver device for engineering modularity in biological networks," *Nature biotechnology*, vol. 32, no. 12, p. 1268, 2014.

[30] Y. Qian and D. D. Vecchio, "Mitigation of ribosome competition through distributed sRNA feedback," in *2016 IEEE 55th Conference on Decision and Control (CDC)*, pp. 758–763, Dec. 2016.

[31] C. Briat, C. Zechner, and M. Khammash, "Design of a synthetic integral feedback circuit: Dynamic analysis and DNA implementation," *ACS Synth. Biol.*, vol. 5, pp. 1108–1116, Oct. 2016.

[32] K. S. Nilgiriwala, J. Jiménez, P. M. Rivera, and D. Del Vecchio, "Synthetic tunable amplifying buffer circuit in e. coli," *ACS synthetic biology*, vol. 4, no. 5, pp. 577–584, 2014.

[33] H.-H. Huang, Y. Qian, and D. Del Vecchio, "A quasi-integral controller for adaptation of genetic modules to variable ribosome demand," *Nature communications*, vol. 9, no. 1, p. 5415, 2018.

[34] U. Alon, *An Introduction to Systems Biology: Design Principles of Biological Circuits*. CRC Press, July 2006. Google-Books-ID: tcxCkIxzCO4C.

[35] Z. Xie, L. Wroblewska, L. Prochazka, R. Weiss, and Y. Benenson, "Multi-input RNAi-based logic circuit for identification of specific cancer cells," *Science*, vol. 333, pp. 1307–1311, Sept. 2011.

[36] Chou Chun Tung, "Detection of persistent signals and its relation to coherent feed-forward loops," *Royal Society Open Science*, vol. 5, p. 181641, Nov. 2018.

[37] N. Farsad, H. B. Yilmaz, A. Eckford, C. Chae, and W. Guo, "A Comprehensive Survey of Recent Advancements in Molecular Communication," *IEEE Communications Surveys Tutorials*, vol. 18, no. 3, pp. 1887–1919, 2016.

[38] L. Grebenstein, J. Kirchner, R. S. Peixoto, W. Zimmermann, F. Irnstorfer, W. Wicke, A. Ahmadzadeh, V. Jamali, G. Fischer, R. Weigel, A. Burkovski, and R. Schober, "Biological Optical-to-Chemical Signal Conversion Interface: A Small-Scale Modulator for Molecular Communications," *IEEE transactions on nanobioscience*, vol. 18, pp. 31–42, Jan. 2019.

[39] A. Marcone, M. Pierobon, and M. Magarini, "Parity-Check Coding Based on Genetic Circuits for Engineered Molecular Communication Between Biological Cells," *IEEE Transactions on Communications*, vol. 66, pp. 6221–6236, Dec. 2018.

[40] S. A. Salehi, H. Jiang, M. D. Riedel, and K. K. Parhi, "Molecular Sensing and Computing Systems," *IEEE Transactions on Molecular, Biological and Multi-Scale Communications*, vol. 1, pp. 249–264, Sept. 2015.

[41] A. Ghodasara and C. A. Voigt, "Balancing gene expression without library construction via a reusable sRNA pool," *Nucleic Acids Research*, vol. 45, pp. 8116–8127, July 2017.

[42] A. Hill, "The possible effects of the aggregation of the molecules of haemoglobin on its dissociation curves," *J Physiol*, vol. 40, pp. iv–vii, 1910.

[43] S. D. Minchin and S. J. Busby, "Analysis of mechanisms of activation and repression at bacterial promoters," *Methods*, vol. 47, no. 1, pp. 6–12, 2009.

[44] C. McBride and D. Del Vecchio, "Analyzing and exploiting the effects of protease sharing in genetic circuits," *IFAC-PapersOnLine*, vol. 50, pp. 10924–10931, July 2017.

[45] D. Del Vecchio, A. J. Ninfa, and E. D. Sontag, "Modular cell biology: retroactivity and insulation," *Mol Syst Biol*, vol. 4, p. 161, Feb. 2008.

[46] M. R. Atkinson, M. A. Savageau, J. T. Myers, and A. J. Ninfa, "Development of genetic circuitry exhibiting toggle switch or oscillatory behavior in Escherichia coli," *Cell*, vol. 113, no. 5, pp. 597–607, 2003.

[47] D. Del Vecchio, "Design and analysis of an activator-repressor clock in e. coli," in *American Control Conference, 2007. ACC'07*, pp. 1589–1594, IEEE, 2007.

[48] S. Jayanthi and D. Del Vecchio, "Tuning genetic clocks employing DNA binding sites," *PLoS One*, vol. 7, no. 7, p. e41019, 2012.

[49] N. S. Kumar and D. Del Vecchio, "Loading as a design parameter for genetic circuits," in *American Control Conference (ACC), 2016*, pp. 7358–7364, IEEE, 2016.

[50] A. Rosenberg, S. Jayanthi, and D. Del Vecchio, "Tuning an activator-repressor clock employing retroactivity," in *American Control Conference (ACC), 2011*, pp. 2308–2313, IEEE, 2011.

[51] J. Saez-Rodriguez, A. Kremling, and E. D. Gilles, "Dissecting the puzzle of life: modularization of signal transduction networks," *Computers & chemical engineering*, vol. 29, no. 3, pp. 619–629, 2005.

[52] H. K. Khalil, *Nonlinear Systems*. Upper Saddle River, N.J: Pearson, 3 edition ed., Dec. 2001.

[53] Y. Kim, M. Coppey, R. Grossman, L. Ajuria, G. Jiménez, Z. Paroush, and S. Y. Shvartsman, "MAPK substrate competition integrates patterning signals in the Drosophila embryo," *Current biology*, vol. 20, no. 5, pp. 446–451, 2010.

[54] Y. Kim, Z. Paroush, K. Nairz, E. Hafen, G. Jiménez, and S. Y. Shvartsman, "Substrate-dependent control of MAPK phosphorylation in vivo," *Molecular systems biology*, vol. 7, no. 1, p. 467, 2011.

[55] R. C. Brewster, F. M. Weinert, H. G. Garcia, D. Song, M. Rydenfelt, and R. Phillips, "The transcription factor titration effect dictates level of gene expression," *Cell*, vol. 156, no. 6, pp. 1312–1323, 2014.

[56] N. E. Buchler and M. Louis, "Molecular titration and ultrasensitivity in regulatory networks," *Journal of molecular biology*, vol. 384, no. 5, pp. 1106–1119, 2008.

[57] N. E. Buchler and F. R. Cross, "Protein sequestration generates a flexible ultrasensitive response in a genetic network," *Molecular systems biology*, vol. 5, no. 1, p. 272, 2009.

[58] T.-H. Lee and N. Maheshri, "A regulatory role for repeated decoy transcription factor binding sites in target gene expression," *Molecular systems biology*, vol. 8, no. 1, p. 576, 2012.

[59] M. L. Wynn, A. C. Ventura, J. A. Sepulchre, H. J. García, and S. D. Merajver, "Kinase inhibitors can produce off-target effects and activate linked pathways by retroactivity," *BMC systems biology*, vol. 5, no. 1, p. 156, 2011.

[60] A. Gyorgy and D. Del Vecchio, "Modular composition of gene transcription networks," *PLoS computational biology*, vol. 10, no. 3, p. e1003486, 2014.

[61] A. C. Ventura, J.-A. Sepulchre, and S. D. Merajver, "A hidden feedback in signaling cascades is revealed," *PLoS computational biology*, vol. 4, no. 3, p. e1000041, 2008.

[62] J.-A. Sepulchre and A. C. Ventura, "Intrinsic feedbacks in MAPK signaling cascades lead to bistability and oscillations," *Acta biotheoretica*, vol. 61, no. 1, pp. 59–78, 2013.

[63] H. R. Ossareh, A. C. Ventura, S. D. Merajver, and D. Del Vecchio, "Long signaling cascades tend to attenuate retroactivity," *Biophysical journal*, vol. 100, no. 7, pp. 1617–1626, 2011.

[64] Y. Qian and D. Del Vecchio, "Effective interaction graphs arising from resource limitations in gene networks," in *2015 American Control Conference (ACC)*, pp. 4417–4423, July 2015.

[65] Y. Qian and D. D. Vecchio, "The "power network" of genetic circuits," in *Emerging Applications of Control and Systems Theory*, Lecture Notes in Control and Information Sciences - Proceedings, pp. 109–121, Springer, Cham, 2018.

[66] M. Carbonell-Ballestero, E. Garcia-Ramallo, R. Montañez, C. Rodriguez-Caso, and J. Macía, "Dealing with the genetic load in bacterial synthetic biology circuits: convergences with the Ohm's law," *Nucleic Acids Res*, vol. 44, pp. 496–507, Jan. 2016.

[67] A. Gyorgy and D. D. Vecchio, "Limitations and trade-offs in gene expression due to competition for shared cellular resources," in *53rd IEEE Conference on Decision and Control*, pp. 5431–5436, Dec. 2014.

[68] F. F. Judd and P. M. Chirlian, "The application of the compensation theorem in the proof of Thevenin's and Norton's theorems," *IEEE Transactions on Education*, vol. 13, pp. 87–88, Aug. 1970.

[69] M. F. Moad, "On Thevenin's and Norton's equivalent circuits," *IEEE Transactions on Education*, vol. 25, pp. 99–102, Aug. 1982.

[70] D. H. Johnson, "Origins of the equivalent circuit concept: the voltage-source equivalent," *Proceedings of the IEEE*, vol. 91, pp. 636–640, Apr. 2003.

[71] K. H. Kim and H. M. Sauro, "Fan-out in gene regulatory networks," *Journal of biological engineering*, vol. 4, no. 1, p. 16, 2010.

[72] K. H. Kim, D. Chandran, and H. M. Sauro, "Toward modularity in synthetic biology: design patterns and fan-out," in *Design and Analysis of Biomolecular Circuits*, pp. 117–138, Springer, 2011.

[73] A. Gyorgy and D. Del Vecchio, "How slaves affect a master module in gene transcription networks," in *Decision and Control (CDC), 2013 IEEE 52nd Annual Conference on*, pp. 6561–6567, IEEE, 2013.

[74] C. McBride and D. Del Vecchio, "Resource sensor design for quantifying competition in genetic circuits," in *57th IEEE Conference on Decision and Control*, Dec. 2018.

[75] R. Shah and D. Del Vecchio, "Signaling architectures that transmit unidirectional information despite retroactivity," *Biophysical journal*, vol. 113, no. 3, pp. 728–742, 2017.

[76] S. Jayanthi and D. Del Vecchio, "Retroactivity attenuation in biomolecular systems based on timescale separation," *IEEE Transactions on Automatic Control*, vol. 56, no. 4, pp. 748–761, 2011.

[77] D. Del Vecchio and S. Jayanthi, "Retroactivity attenuation in transcriptional networks: Design and analysis of an insulation device," in *Decision and Control, 2008. CDC 2008. 47th IEEE Conference on*, pp. 774–780, IEEE, 2008.

[78] P. M. Rivera and D. Del Vecchio, "Optimal design of phosphorylation-based insulation devices," in *American Control Conference (ACC), 2013*, pp. 3783–3789, IEEE, 2013.

[79] R. Shah and D. Del Vecchio, "An n-stage cascade of phosphorylation cycles as an insulation device for synthetic biological circuits," in *Control Conference (ECC), 2016 European*, pp. 1832–1837, IEEE, 2016.

[80] C. Briat, A. Gupta, and M. Khammash, "Antithetic integral feedback ensures robust perfect adaptation in noisy biomolecular networks," *cels*, vol. 2, pp. 15–26, Jan. 2016.

[81] E. Levine, Z. Zhang, T. Kuhlman, and T. Hwa, "Quantitative Characteristics of Gene Regulation by Small RNA," *PLOS Biology*, vol. 5, Aug. 2007.

[82] Y. Qian and D. Del Vecchio, "Realizing 'integral control' in living cells: how to overcome leaky integration due to dilution?," *J R Soc Interface*, vol. 15, Feb. 2018.

[83] M. Vidyasagar, *Input-Output Analysis of Large-Scale Interconnected Systems: Decomposition, Well-Posedness and Stability*. Lecture Notes in Control and Information Sciences, Berlin Heidelberg: Springer-Verlag, 1981.

[84] J. Ang and D. R. McMillen, "Physical constraints on biological integral control design for homeostasis and sensory adaptation," *Biophys. J.*, vol. 104, pp. 505–515, Jan. 2013.

[85] T. Shopera, L. He, T. Oyetunde, Y. J. Tang, and T. S. Moon, "Decoupling resource-coupled gene expression in living cells," *ACS Synth. Biol.*, vol. 6, pp. 1596–1604, Aug. 2017.

[86] A. P. S. Darlington, J. Kim, J. I. Jiménez, and D. G. Bates, "Dynamic allocation of orthogonal ribosomes facilitates uncoupling of co-expressed genes," *Nature Communications*, vol. 9, p. 695, Feb. 2018.

[87] D. Del Vecchio, Y. Qian, R. M. Murray, and E. D. Sontag, "Future systems and control research in synthetic biology," *Annual Reviews in Control*, vol. 45, pp. 5–17, Jan. 2018.

APPENDIX

A. Modeling transcription-translation (TX/TL) processes

Here we describe the standard ODE models derived from first principles for the TX/TL process in more detail. As in Fig. 1a, DNA makes an mRNA template through transcription (TX) and the mRNA template makes a protein through translation (TL). This situation is described by the set of reactions

$$\begin{aligned} \mathrm{D}_i + \mathrm{RNAP} + \mathrm{u} \underset{a_{1i}}{\overset{d_{1i}}{\rightleftharpoons}} \mathrm{C}_{1i} \xrightarrow{k_{1i}} \mathrm{m}_i + \mathrm{D}_i + \mathrm{RNAP} + \mathrm{u}_i \\ \mathrm{m}_i + \mathrm{Ribo} \underset{a_{1i}}{\overset{d_{2i}}{\rightleftharpoons}} \mathrm{C}_{2i} \xrightarrow{k_{2i}} \mathrm{x}_i + \mathrm{m}_i + \mathrm{Ribo} \\ \mathrm{m}_i \xrightarrow{\delta} \emptyset \qquad \mathrm{x}_i \xrightarrow{\gamma} \emptyset. \end{aligned} \tag{19}$$

Then, using the law of mass action, the set of ODEs describing the TX/TL node dynamics is given as

$$\dot{C}_{1i} = a_{1i} D_i u RNAP - (d_{1i} + k_{1i}) C_{1i} \tag{20a}$$

$$\dot{m}_i = k_{1i} C_{1i} - \delta m_i \tag{20b}$$

$$\dot{C}_{2i} = a_{2i} m_i Ribo - (d_{2i} + k_{2i}) C_{2i} \tag{20c}$$

$$\dot{x}_i = k_{2i} C_{2i} - \gamma x_i. \tag{20d}$$

It can be shown that the species D_i, and Ribo obey the conservation laws

$$D_{tot_i} = D_i + C_{1i} \tag{21a}$$

$$Ribo_{tot} = Ribo + \sum_i C_{2i} \tag{21b}$$

where D_{tot_i} is the total concentration of DNA for the ith node, $Ribo_{tot}$ is the total concentration of the ribosomes. We assume that the RNAP resource is non-limiting, which has been shown to be a valid assumption in *E. coli* [27], so we assume that $RNAP$ is a constant. These conservation laws may be used to substitute into (20). Timescale separation may be applied to reduce the model since the dynamics of C_{1i} and C_{2i} are much faster than the dynamics of x_i or m_i for all i. Then, (20) may be reduced two states for each TX/TL process. Specifically, the set of ODEs describing the two nodes in Fig. 6 is given as

$$\dot{m}_1 = T_1 \frac{\beta + (u/K)^n}{1 + (u/K)^n} - \delta m_1 \tag{22a}$$

$$\dot{x}_1 = R_1 \frac{m_1/\kappa_1}{1 + \alpha(m_1/\kappa_1 + m_2/\kappa_2)} - \gamma x_1 \tag{22b}$$

$$\dot{m}_2 = T_2 - \delta m_2 \tag{22c}$$

$$\dot{x}_2 = R_2 \frac{m_2/\kappa_2}{1 + \alpha(m_1/\kappa_1 + m_2/\kappa_2)} - \gamma x_2 \tag{22d}$$

with the outputs of each node given as $y_1 = x_1$ and $y_2 = x_2$. Here, $T_i = k_{1i} RNAP$ represents the maximum rate of mRNA production, β represents the leaky transcription of the DNA, $K = \frac{d_{1i}+k_{1i}}{a_{1i}}$ represents the binding constant between the input u and the DNA, n represents the cooperativity of the input u, $R_i = k_{2i} Ribo_{tot}$ represents the maximum rate of protein production, and $\kappa_i = \frac{d_{2i}+k_{2i}}{a_{2i}}$ represents the binding constant between mRNA and ribosomes. The system in (22) was simulated by observing the steady state for different values of the input u, shown in Fig. 6. The parameters used in this simulation are given in Table I. For the system without resource sharing, $\alpha = 0$ and for the system with resource sharing, $\alpha = 1$.

TABLE I
PARAMETERS USED IN THE SIMULATIONS OF (22) IN FIG. 6.

T_1	T_2	β	K	n	R_1	R_2	κ_1, κ_2	δ	γ
1000	100	0.001	1	2	100	1000	1000	5	1

Similar modeling techniques are used when a given TX/TL node takes two inputs, for example an activator and a repressor. For details, the reader is referred to [5]. The equations governing the activator-repressor clock in Fig. 2 are

$$\begin{aligned}\dot{A} &= \frac{\alpha_1 + \beta_1 A^n}{1 + A^n + R^n} - \delta_A A - k_{on} A(p_T - C) + k_{off} C,\\ \dot{R} &= \frac{\alpha_2 + \beta_2 A^n}{1 + A^n} - \delta_R R,\\ \dot{C} &= k_{\text{on}} A(p_T - C) - k_{\text{off}} C.\end{aligned} \tag{23}$$

Here, A is the concentration of the activator, R is the concentration of the repressor, and C is the concentration of the complex formed by the activator and the downstream DNA sites. The parameters used for the simulations of the clock are given in Table A. For the unloaded clock $p_T = 0$, and $p_T = 150$ for the loaded clock.

TABLE II
PARAMETERS USED IN THE SIMULATIONS OF (23) IN FIG. 2

α_1	β_1	α_2	β_2	n	δ_A	δ_R	k_{on}	k_{off}
0.04	300	0.004	300	2	1	0.5	10	100

B. Modeling sRNA dynamics

The chemical reactions governing sRNA degradation of mRNA is given as

$$\begin{gathered}\mathrm{s}_i + \mathrm{m}_i \underset{a_{si}}{\overset{d_{si}}{\rightleftharpoons}} \mathrm{C}_i \xrightarrow{k_{si}} \emptyset\\ \mathrm{s}_i \xrightarrow{\delta} \emptyset.\end{gathered} \tag{24}$$

These reactions may augment the reactions for the rest of the network such as those given in (19). Using techniques presented in Appendix A, a set of ODEs may be used to model the system. The reduced set of ODEs that describe the sRNA feedback controller around each node for two unconnected nodes as in Fig. 14 are

$$\begin{aligned}\dot{m}_1 &= GT_1 \frac{\beta + (u/K)^n}{1 + (u/K)^n} - Gm_1 s_1 - \delta m_1\\ \dot{s}_1 &= GT_{s1} \frac{x_1/K_{s1}}{1 + x_1/K_{s1}} - Gm_1 s_1 - \delta s_1\\ \dot{x}_1 &= R_1 \frac{m_1/\kappa_1}{1 + \alpha(m_1/\kappa_1 + m_2/\kappa_2)} - \gamma x_1\\ \dot{m}_2 &= GT_2 - Gm_2 s_2 - \delta m_2\\ \dot{s}_2 &= GT_{s2} \frac{x_2/K_{s2}}{1 + x_2/K_{s2}} - Gm_2 s_2 - \delta s_2\\ \dot{x}_2 &= R_2 \frac{m_2/\kappa_1}{1 + \alpha(m_1/\kappa_1 + m_2/\kappa_2)} - \gamma x_2\end{aligned}$$

where $G = \frac{k_{si}}{d_{si}/a_{si}}$, which is assumed to be the same for all i. For a detailed derivation of this model, the reader is referred to [30]. Parameters used to simulate this system are given in Tables I and III.

TABLE III
PARAMETERS USED IN THE SIMULATION OF (25) SHOWN IN FIG. 14B ALONG WITH THE PARAMETERS IN TABLE I.

T_{s1}, T_{s2}	K_{s1}, K_{s2}
1200	10

C. Modeling phosphorylation-dephosphorylation cycles

In this section, we describe the reactions that make up a single phosphorylation-dephosphorylation cycle (Fig. 15), and explain how these reactions can be used to develop the ordinary differential equation (ODE) model for the cycle based on reaction-rate equations. Models of multi-stage cycles can be developed by composing many models of the single cycle, and the procedure for doing so is described in brief.

Consider a single phosphorylation cycle with kinase Z, substrate X, and phosphatase M, as shown in Fig. 15. Kinase Z enzymatically converts substrate X to phosphorylated protein X^* by means of a two-strep reaction with an intermediate complex C_1, as follows:

$$\mathrm{Z} + \mathrm{X} \underset{d_1}{\overset{a_1}{\rightleftharpoons}} \mathrm{C}_1 \xrightarrow{k_1} \mathrm{X}^* + \mathrm{Z}. \tag{26}$$

Here, a_1 is the binding rate of Z and X, d_1 is the unbinding rate of Z and X, and k_1 is the rate of production of the phosphorylated protein X^* from the complex C_1.

Similarly, the phosphatase M enzymatically converts the phosphorylated protein X^* back to the dephosphorylated substrate X by means of the two-step reaction

$$\mathrm{M} + \mathrm{X}^* \underset{d_2}{\overset{a_2}{\rightleftharpoons}} \mathrm{C}_2 \xrightarrow{k_2} \mathrm{X} + \mathrm{M}. \tag{27}$$

The cycle can then be modeled in the form of a set of ODEs,

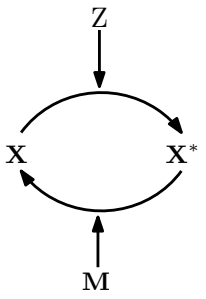

Fig. 15. A single phosphorylation cycle with kinase Z, substrate X, phosphorylated substrate X^*, and phosphatase M.

where the state variables are the concentrations Z, X, X^*, M, C_1 and C_2 of the species Z, X, X^*, M, C_1 and C_2, respectively. The set of ODEs for this cycle are then:

$$\begin{aligned}\dot{Z} &= -a_1 ZX + (d_1 + k_1)C_1,\\ \dot{X} &= -a_1 ZX + d_1 C_1 + k_2 C_2,\\ \dot{X}^* &= k_1 C_1 - a_2 M X^* + d_2 C_2,\\ \dot{M} &= -a_2 M X^* + (d_2 + k_2)C_2,\\ \dot{C}_1 &= a_1 ZX - (d_1 + k_1)C_1,\\ \dot{C}_2 &= a_2 M X^* - (d_2 + k_2)C_2,\end{aligned} \tag{28}$$

where the parameters are the reaction-rate constants $a_1, d_1, k_1, a_2, d_2, k_2$. Note that these dynamics are added to any other terms arising from other reactions the species might participate in, as well as any production or decay terms. For example, if kinase Z is produced by a TX/TL process with production rate given by the Hill function $H(u)$ and decays with rate δ, then the ODE governing the dynamics of Z become:

$$\dot{Z} = H(u) - \delta Z - a_1 ZX + (d_1 + k_1)C_1.$$

The set of ODEs in (28) can be reduced by conservation laws. For example, the total concentration of the phosphatase can be assumed to be constant, that is, $M_T = M + C_2$ where M_T represents the total concentration of phosphatase and is constant. Then, the dynamics of M can be eliminated by replacing $M = M_T - C_2$ in the system of equations. Models for multi-stage phosphorylation cycles can be constructed by composing models of single phosphorylation cycles. For example, the cycle described in (28) can drive another phosphorylation cycle where X^* acts as the kinase for the phosphorylation of the substrate of the second cycle Y. The dynamics of species shared by both cycles (in this case, for example X^*) consist all the reaction-rate terms from the reactions they participate in across both the cycles.

For the two-stage phosphorylation cycle insulation device connected between the clock and the downstream TX/TL node, the set of ODEs describing the model are

$$\begin{aligned}
\dot{A} &= \frac{\alpha_1 + \beta_1 A^n}{1 + A^n + R^n} - \delta_A A - a_1 X_1 A + (d_1 + k_1)C_1,\\
\dot{R} &= \frac{\alpha_2 + \beta_2 A^n}{1 + A^n} - \delta_R R,\\
\dot{X}_1^* &= k_1 C_1 - a_2 M_1 X_1^* + d_2 C_2,\\
\dot{M}_1 &= -a_2 M_1 X_1^* + (d_2 + k_2)C_2,\\
\dot{C}_1 &= a_1 A X_1 - (d_1 + k_1)C_1,\\
\dot{C}_2 &= a_2 M_1 X_1^* - (d_2 + k_2)C_2,\\
\dot{C}_3 &= a_3 X_1^* X_2 - (d_3 + k_3)C_3,\\
\dot{C}_4 &= a_4 X_2^* M_2 - (d_4 + k_4)C_4,\\
\dot{X}_2^* &= k_3 C_3 - a_4 X_2^* M_2 + d_4 C_4 - k_{\text{on}} X_2^* (p_T - C) + k_{\text{off}} C,\\
\dot{C} &= k_{\text{on}} X_2^* (p_T - C) - k_{\text{off}} C,\\
X_1 &= X_{T1} - C_1 - X_1^* - C_2 - C_3,\\
X_2 &= X_{T2} - X_2^* - C_3 - C_4 - C,\\
M_1 &= M_{T1} - C_2,\\
M_2 &= M_{T2} - C_4.
\end{aligned} \tag{29}$$

The parameters used for the insulation device in Fig. 11 are given in Table C.

TABLE IV
PARAMETERS USED IN THE SIMULATIONS OF (29) SHOWN IN FIG. 11 ALONG WITH THE PARAMETERS GIVEN IN TABLE A.

X_{T1}	M_{T1}	X_{T2}	M_{T2}	a_i	d_i	k_i
3	100	1000	30	18	2400	600